DOI: 10.1002/adsc.200600346

Phosphinite Ligand Effects in Palladium(II)-Catalysed Cycloisomerisation of 1,6-Dienes: Bicyclo[3.2.0]heptanyl Diphosphinite (B[3.2.0]DPO) Ligands Exhibit Flexible Bite Angles, an Effect Derived from Conformational Changes (*exo*- or *endo*-Envelope) in the Bicyclic Ligand Scaffold

Ian J. S. Fairlamb,[a,*] Stephanie Grant,[a] Simona Tommasi,[a,b] Jason M. Lynam,[a] Marco Bandini,[b] Hao Dong,[c] Zhenyang Lin,[c] and Adrian C. Whitwood[a]

[a] Department of Chemistry, University of York, Heslington, York, YO10 5DD, UK
Fax: (+44)-1904-432-515; e-mail: ijsf1@york.ac.uk
[b] Dipartimento di Chimica "G. Ciamician", Via Selmi 2, 40126, Bologna, Italy
[c] Department of Chemistry, The Hong Kong University of Science and Technology, Clear Water Bay, Kowloon, Hong Kong, People's Republic of China

Received: July 12, 2006; Accepted: September 13, 2006

Abstract: Changes in bidentate ligand structure significantly affect catalytic activity in mono-cationic Pd(II)-catalysed 1,6-diene cycloisomerisation processes to give cyclopentene products. A bicyclo[3.2.0]heptanyl diphosphinite ligand (B[3.2.0]DPO, **3**) is the first phosphorus-based bidentate ligand capable of promoting regioselective 1,6-diene cycloisomerisation. Trace quantities of water are essential for catalytic activity, as is the precise order of mixing of 1,6-diene, Pd(II) pro-catalyst and additives. Conformational changes in the ligand backbone seem to be important in stabilising the active catalyst species, assumed to be a cationic Pd(II) hydride species. DFT calculations support a change in bite angle on the cationic Pd(II) hydride species from circa 90° (*cis*) to 170° (*trans*); in the latter geometry an agostic interaction of the C4 *endo* hydrogen of the bicyclic ring-system with Pd(II) stabilises the cationic metal centre. This unique ligand property could be exploited in other transition metal catalysed processes.

Keywords: anion effects; C–C bond formation; cyclization; isomerization; palladium

Introduction

The transition metal-catalysed cycloisomerisation of 1,6-dienes (**1**→**2a–c**) is a powerful, atom-economic and environmentally benign method for the efficient synthesis of carbo- and heterocyclic compounds (Scheme 1);[1] the resultant cyclised products are most commonly five-membered ring systems (**2a–c**) (**1′** is occasionally seen as a side-product).

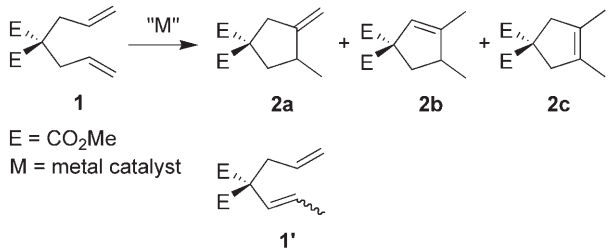

Scheme 1. Products from 1,6-diene cycloisomerisation.

Several transition metals are known to promote 1,6-diene cycloisomerisation (Ti,[2] Rh,[3] Ru,[4] Ni,[5] Pd[6]), and in the majority of reports, individual catalyst systems have been developed permitting regioselective cycloisomerisation for one of the regioisomeric products **2a–c**. In terms of synthetic utility, Gagné and co-workers have studied $[(triphos)Pt(II)]^+$ carbophilic Lewis acid catalysts which cycloisomerise structurally diverse 1,6-diene substrates to give terpenoid natural products and related derivatives [triphos = $CH_3C(CH_2PPh_2)_3$].[7] Recently, asymmetric 1,6-diene cycloisomerisation processes have begun to emerge as potentially valuable synthetic strategies. Specifically, chiral Pd[8] or Ni[9] catalysts have been reported. For the former, a catalyst system consisting of $(CH_3CN)_2PdCl_2$/2 $AgBF_4$/(*R*,*R*)-4,4′-dibenzylbisoxazoline or (−)-sparteine, gave promising enantiomeric

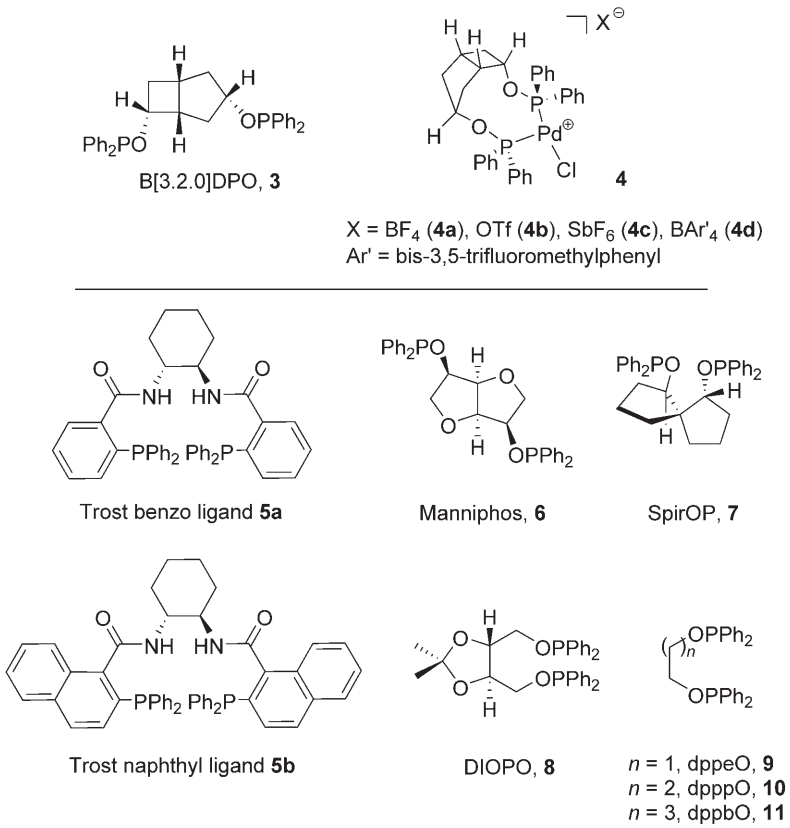

Figure 1. Phosphinite ligands for 1,6-diene cycloisomerisation.

excesses (*ee*s) up to 60% for **2b** (37% for **2a**), although conversions and regioselectivities remained low (**2a**:**2b**, 1:1.1). In order to utilise Pd(II) catalysts/procatalysts in asymmetric 1,6-diene cycloisomerisation processes, it is essential that the regioselectivity be controlled, in essence this is a *mandatory requirement*. It was speculated that it ought to be possible to utilise readily available chiral phosphine or phosphinite ligands to promote a regio- and enantioselective process. We have screened many commercially available chiral bidentate phosphine ligands, e.g., Trost modular ligands **5a** and **5b**,[10] Manniphos **6**,[11] SpirOP **7**[12] and DIOPO **8**, as well as non-chiral ligands **9**–**11**, in combination with catalytic Pd(II) (neutral or cationic), for the cycloisomerisation of **1**, which generally exhibited poor catalytic activity. The unique bidentate phosphinite ligand **3** (B[3.2.0]DPO),[13] containing a bicyclo[3.2.0]heptanyl skeleton and two phosphinite donors at C3 and C6 in an *endo*-orientation, in combination with monocationic Pd(II) (as **4**), was then shown to promote the regioselective cycloisomerisation of **1** to give **2b** (>90% isomer selectivity) (Figure 1).[14] Remarkable effects on the regioselectivity were broadly seen with BAr'_4, BF_4, OTf and SbF_6 anions. The best combination of catalytic activity and regioselectivity was found for the non-coordinating BAr'_4 anion (Ar′ = bis-3,5-trifluoromethylphenyl). In this full paper our comprehensive studies on the cycloisomerisation activity of **4a**–**d** are reported. The importance of the bicyclo[3.2.0]heptane skeleton is elaborated upon, revealing that B[3.2.0]DPO is an exceptional ligand for this reaction. DFT calculations, NMR spectroscopic and X-ray diffraction studies provide evidence that B[3.2.0]DPO ligands are flexible enough to allow changes in bite angle around the metal centre, which could be important in stabilisation of the active catalyst species, thought to be a cationic Pd(II) hydride.

Results and Discussion

In an initial benchmark reaction a catalytic amount of [(B[3.2.0]DPO)$PdCl_2$] (5 mol%) was added to either an anhydrous or reagent-grade DCE solution containing dimethyl diallylmalonate **1** at 40, 60 and 80°C. However, under these conditions negligible cycloisomerisation was observed after 48 h; note that procatalysts, e.g., $(RCN)_2PdCl_2$ (where R = *t*-butyl, methyl or phenyl), developed by Lloyd-Jones and co-workers, are particularly active under identical reaction conditions.[6b] There are several other Pd(II) procatalysts reported for this reaction where a cationic Pd(II) species is believed to be important.[1c,6c] The above cycloi-

Table 1. Anion effects in Pd(II)-catalysed cycloisomerisation of **1**→**2a–c**.[a]

Entry	Additive	Reaction time [hours] 4	24
1	-	100/0/0/0	98/1/2/0
2	AgOTf [5 mol%]	5/0/14/46[b]	8/0/5/57[c]
3	$NaBAr'_4$ [5 mol%]	46/0/54/0	0/0/95/5
4	$AgBF_4$ [5 mol%]	90/0/10/0	63/0/37/0
5	$AgSbF_6$ [5 mol%]	90/0/10/0	72/0/27/1
6	AgOTf [10 mol%]	0/0/5/53[d]	-
7	$NaBAr'_4$ [10 mol%]	18/9/30/6[e]	-

[a] *Reaction conditions* (reaction as given in Scheme 1): **1** ($c=0.236$ M), [(B[3.2.0]DPO)$PdCl_2$] (5 mol%), DCE, 60°C; Ratio of **1**/**2a**/**2b**/**2c** was determined by ^{1}H NMR spectroscopy.
[b] Isomerised **1′** (35%) detected.
[c] Isomerised **1′** (30%) detected.
[d] Isomerised **1′** (37%) detected.
[e] Isomerised **1′** (42%) detected.

somerisation reaction was conducted using one equivalent of either AgOTf, $AgBF_4$, $AgSbF_6$ and $NaBAr'_4$, with respect to [(B[3.2.0]DPO)$PdCl_2$], in DCE at 60°C (Table 1).

Pronounced anion effects are seen in Table 1. The *exo*-methylenecyclopentene kinetic product **2a** was not detected for any of the additives investigated at 60°C (**2a** is seen in small quantities at 40°C).[14] In the presence of the OTf anion, cyclopentenyl product **2b** is isomerised to **2c** after 24 h (entry 2). Isomerisation of **1** to **1′** was found for the OTf anion, which is most likely initiated by the presence of triflic acid, a common side-product formed from reaction of adventitious H_2O and $[L_nPd]^+[OTf]^-$, which could also isomerise **2b** to **2c**.[1c] The best combination of selectivity and activity was established with the BAr'_4 anion, which after 24 h gave predominately **2b** (95% selectivity; entry 3). In terms of selectivity, the more coordinating BF_4 anion produces **2b** exclusively, at the expense of higher conversion (entry 4). Only after 72 h is the more thermodynamically stable symmetrical product **2c** observed ($AgBF_4$, 60°C, 72 h; **1**/**2b**/**2c**, 26/73/1). For the SbF_6 anion catalytic activity is comparable with the BF_4 anion, although a trace quantity of **2c** is detected after 24 h (entry 5). Running reactions with two equivalents of AgOTf or $NaBAr'_4$ with respect to [(B[3.2.0]DPO)$PdCl_2$] in DCE at 60°C resulted in higher catalytic activity (entries 6 and 7). For the former OTf anion, the reaction was complete after 4 h (entry 6); for the latter BAr'_4 anion, only 18% of **1** remained after 4 h and a mixture of products **2a–c** (entry 7). Extensive isomerisation of **1** to **1′** was seen for both cases. Crucially, it appears that halide redistribution[15] is absent in this catalyst system, e.g., the monocationic species [(B[3.2.0]DPO)PdCl]$^+$[X]$^-$ is not in equilibrium with [(B[3.2.0]DPO)$PdCl_2$] and {[(B[3.2.0]DPO)Pd]$^{2+}$[X]$_2^{2-}$} at the catalyst/substrate concentrations employed in these experiments. Such phenomena are apparent with other cationic Pd(II) catalysts/procatalysts;[8] one would anticipate a less striking outcome to that observed, on both catalytic activity and selectivity, on comparison of the neutral, +1 and +2 cationic species.

The order of mixing of reagents appears to be important. If the metal salt was added first to [(B[3.2.0]DPO)$PdCl_2$] in DCE to generate [(B[3.2.0]DPO)PdCl]$^+$[X]$^-$, followed by 1,6-diene **1**, the reactions were sluggish. After some experimentation, it was found that **1** should be dissolved first in DCE in a vial and then transferred to the reaction vessel, and then [(B[3.2.0]DPO)$PdCl_2$] added, followed *immediately* by the metal salt (under N_2 atmosphere). The reaction was then heated to 60°C. A very slight colour change is observed from a pale yellow to a brighter yellow on addition of the metal salt; the precipitation of AgCl is apparent (solutions appear cloudy where NaCl is formed).

We next investigated the evolution of products **2b** and **2c**, mediated by the [(B[3.2.0]DPO)$PdCl_2$]/$NaBAr'_4$ (1:1, 5 mol%) catalyst system in reagent grade DCE at 60°C, which is shown in Figure 2. Significantly, the kinetic profile exhibits the absence of an induction period (the reaction is slowed significantly in anhydrous DCE, purity >99.9%; conducted in a dry-box at O_2 levels <1 ppm). Prolonged reaction to 72 h shows negligible isomerisation of **2b** to **2c** (remains at ~95:5; as shown by ^{1}H NMR spectroscopy). The selective formation of **2b** is seen up to ~50% conversion (4 h) and it is at this point that isomerisation to **2c** becomes noticeable. Analysis of the reaction kinetics reveals that the consumption of **1** follows pseudo first-order behaviour, $k_{obs}=(3.90\pm0.15)\times10^{-5}\,s^{-1}$ (see later for discussion).

Changing the solvent from DCE to CH_3CN under the optimum conditions, namely [(B[3.2.0]DPO)$PdCl_2$]/$NaBAr'_4$ (1:1, 5 mol%) at 60°C, resulted in a decrease in cycloisomerisation rate (6% conversion to **2b**, 100% selectivity after 4 h). Competitive CH_3CN coordination for monocationic Pd(II) presumably accounts for this finding.

Heating **2a**, independently prepared by cycloisomerisation of **1** using [Ru(cod)Cl]$_n$ in *i*-PrOH at reflux, 89% **2a** by ^{1}H NMR spectroscopy (containing ~11% **2b**),[4a] in the presence of [(B[3.2.0]DPO)$PdCl_2$]/$NaBAr'_4$ (1:1, 5 mol%) at 60°C results in cycloisomerisation to the stable thermodynamic products **2b** and **2c** (Table 2). The *exo*-methylenecyclopentene **2a** was isomerised to both **2b** and **2c**. We also assessed whether [(B[3.2.0]DPO)PdCl]$^+$-[BAr'_4]$^-$ could catalyse the cycloisomerisation of **1** after isomerising **2a** to **2b** and **2c**. Indeed, this proved to be a highly reactive catalyst system, and 2 h after

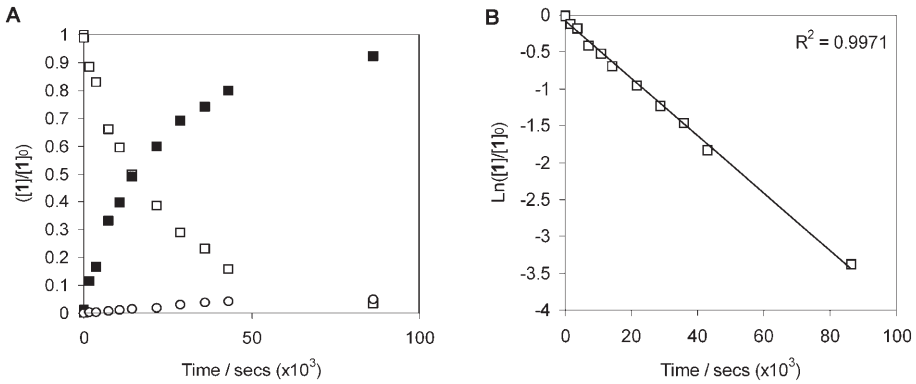

Figure 2. A: Kinetic profile for the cycloisomerisation of dimethyl diallylmalonate **1**[38] by [(B[3.2.0]DPO)PdCl$_2$] (5 mol%), NaBAr′$_4$ (5 mol%), DCE, 60°C; monitored by ^{1}H NMR spectroscopy (400 MHz); [**1**] at t_0=0.245 M. Key: □, 1,6-diene **1**; ■, endocyclic product **2b**; ○, cyclopentenyl product **2c. B**: Pseudo first-order kinetics for loss of 1,6-diene **1** {k_{obs}=(3.90±0.15)×10^{-5} s^{-1}}.

addition of **1** (26 h) complete consumption was found, affording a mixture of **2a–c**, in favour of **2b**. After a further 24 h (50 h), **2a** had disappeared, isomerised to **2b**; note that the proportion of **2c** remains constant. In a separate experiment, heating **2b** exhibited slow isomerisation to **2c** over 24 h. As for **2a**, the addition of **1** resulted in rapid cycloisomerisation, affording initially **2a**, in addition to **2b** and small quantities of **2c** after 2 h (26 h). After a further 24 h (50 h) the ratio of **2b**:**2c** was 93:7.

Anion Effects

There is a possibility that cycloisomerisation of **1** could be promoted by a strong Lewis acid such as SbF$_5$ derived from HSbF$_6$ {formed by reaction of [(B-[3.2.0]DPO)PdCl]$^+$[SbF$_6$]$^-$ and H$_2$O}. Mechanistically, it would seem plausible that six-membered ring products ought to be formed under such Lewis acid catalysis, if a selective process could be identified.[16] Of note is the finding that reactions mediated by catalytic quantities of SbF$_5$ did not promote cycloisomerisation. Instead, some isomerisation of 1,6-diene **1**→**1′** occurred, in addition to a second more dominant reaction pathway; the resultant product(s) from the latter reaction showed loss of the alkenyl proton and ester methyl proton resonances in the ^{1}H NMR spectrum, although it appeared that a mixture of diastereoisomeric products had been formed, *ca.* 1:1:2.5 (Scheme 2).

A crystal from this reaction was selected for study by X-ray diffraction, which confirmed that spirodilactonisation had taken place to afford **12** (Figure 3). The stereochemical course of the reaction may lead to the formation of three diastereoisomers; the relative orientation of the substituents on the spiro-fused lactones may be defined as symmetrical-*syn*, unsymmetrical and symmetrical-*anti*.[17] The X-ray structure confirms the stereochemistry as the symmetrical-*syn* diastereoisomer, which occupies an unusual higher

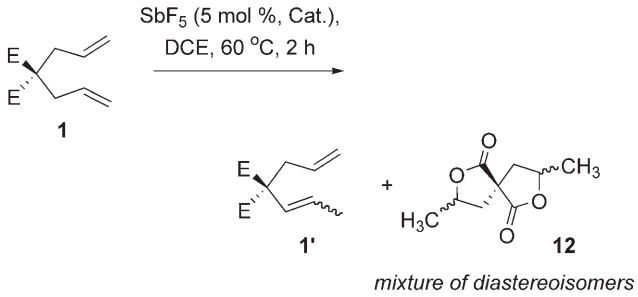

Scheme 2. Reaction of **1** with catalytic SbF$_5$.

Table 2. Further isomerisation of **2a** and **2b** by monocationic Pd(II).[a]

Cyclic product	Reaction time [hours] 0	2	4	24		26	50
2a	0/89/11/0	0/63/18/19	0/59/19/22	0/24/36/40	1 equiv. of 1,6-diene **1** added	0/15/54/31	0/0/66/34
2b	0/0/97/3	0/0/95/5	0/0/95/5	0/091/9		0/5/88/7	0/0/93/7

[a] *Reaction conditions*: Cycloisomerisation product **2a** or **2b** (c=0.245 M), [(B[3.2.0]DPO)PdCl$_2$] (5 mol%), NaBAr′$_4$ (5 mol%), DCE, 60°C; after 24 h 1 equiv. of **1** with respect to **2a** or **2b** was added to the reaction mixture; Ratio of **1**/**2a**/**2b**/**2c** was determined by ^{1}H NMR spectroscopy.

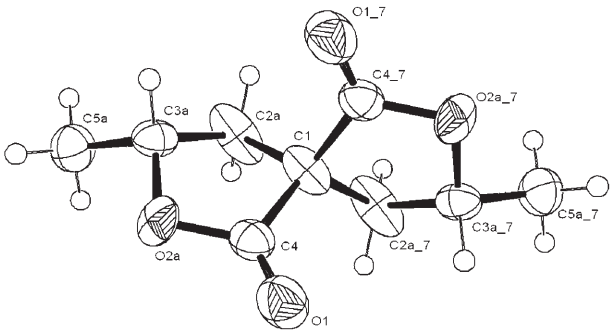

Figure 3. X-ray crystal structure of spirocycle **12**.

order symmetry space group, $P4_32_12$.[18] ^{1}H NMR spectroscopic analysis of the crystals, in comparison with the ^{1}H NMR spectrum of the crude material, confirmed that this was the major diastereoisomer; the minor diastereoisomers seen in the crude reaction mixture are thus the symmetrical-*anti* and unsymmetrical compounds.[18] The formation of **12** can be rationalised through consideration of the mechanism provided in Scheme 3. Addition of SbF_5 to the terminal alkene generates secondary carbocation intermediate **I**, which could potentially be trapped by the tethered alkene, however *O*-attack is evidently preferred to give **II**. Loss of MeX (e.g., X = Cl) affords cycloadduct **III** which can then react with a proton to generate the initial lactone product **13**, which re-enters the cycle once more to give spirocycle **12**. It is highly likely that SbF_5 also reacts with DCE to give HCl amongst other products, but HCl is produced from DCE on prolonged heating at 60 °C in the presence of trace quantities of H_2O.[19] The super-acid $HSbF_5OH$ could also be formed under the reaction conditions, which hydrolyses the esters first, which is then followed by a more classical cyclisation process (alkene protonation/carboxylate trapping of the resultant carbocation).

Substrate Scope

Several 1,6-dienes were effectively cycloisomerised with the [(B[3.2.0]DPO)$PdCl_2$]/$NaBAr'_4$ (5 mol%) catalyst system (Table 3), which was generally effective providing that the 1,6-diene possessed a carbon tether. Diethyl diallylmalonate **14** gave the cyclopentenyl product **15** in > 99% yield, in similar selectivity to **2b** (entries 1 and 2). Selective cycloisomerisations were also recorded for the pro-spirobicyclic 1,6-dienes **16** and **18**, to give spirobicycles **17** and **19** in > 99% and 45% yields, respectively (entries 3 and 4). Disappointingly, substitution of the alkenyl moiety of **1**, as in **20** and **22**, resulted in a dramatic loss of catalytic activity (entries 5 and 6).

Effect of Ligand Backbone

Given that the reaction conditions would be conducive to the formation of HCl *vide supra*, we were keen to test whether elimination of the bicyclic backbone occurred in [(B[3.2.0]DPO)$PdCl_2$] (or the monocationic species derived from reaction with MX) in DCE. For certain types of phosphinites, oxygen protonation leads to facile elimination to generate the so-called[20] POPd dimer complex **24** (Figure 4). Indeed we[14] and other groups[21] have observed deleterious degradation pathways for several monophosphinite ligands in CH_2Cl_2, $CHCl_3$ and DCE, and although it does occur for certain bidentate and multidentate

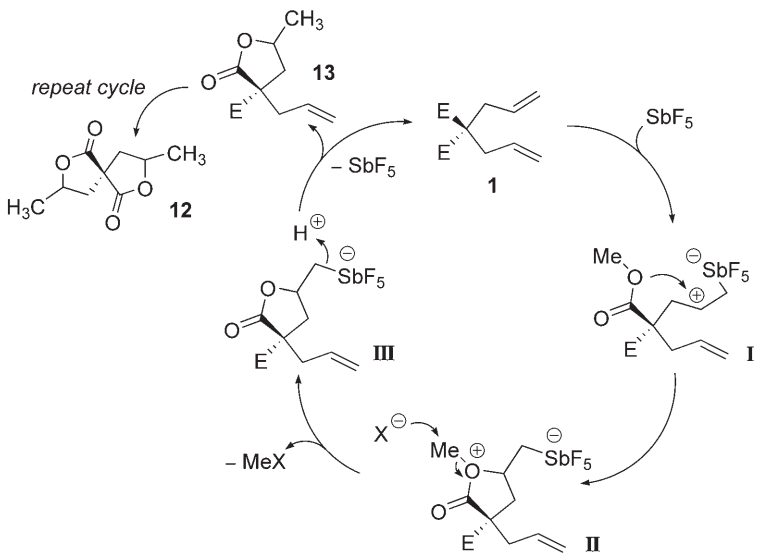

Scheme 3. Mechanism to account for the formation of spirocycle **12**.

Table 3. Substrate scope for 1,6-diene cycloisomerisation reactions mediated by [(B[3.2.0]DPO)PdCl$_2$]/NaBAr′$_4$ (5 mol%) in DCE at 60°C for 24 h.[a]

Entry	1,6-Diene		Cycloisomerisation product		Yield [%][b]	Selectivity [%][c]
1	**1**	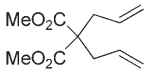	**2b**	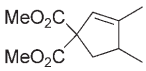	94	95
2	**14**	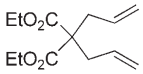	**15**	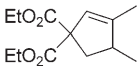	>99	93
3	**16**	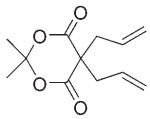	**17**	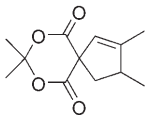	>99	76
4	**18**	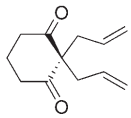	**19**	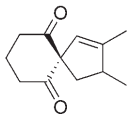	45	66
5	**20**	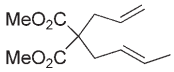	**21**	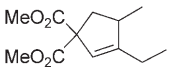	4[d]	>99
6	**22**	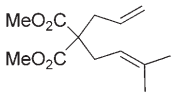	**23**	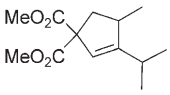	8[d]	>99

[a] Reactions were monitored by either ^{1}H NMR spectroscopy, GC and/or GC/MS (where appropriate).
[b] Yields are after purification by column chromatography.
[c] Selectivity determined by ^{1}H NMR spectroscopy of the crude reaction material. The regioisomeric cyclopentenyl products cannot be separated by chromatography.
[d] These numbers represent % conversion. We were unable to fully characterise these cyclic products, given the low conversions (separation of **20** from **21**, and **22** from **23**, was not possible – identical R_f values). However, new alkenic signals, consistent with structures **21** and **23** were observed by ^{1}H and ^{13}C NMR spectroscopy (the position of the trisubstituted alkene can be explained by the mechanism shown in Scheme 8; see later).

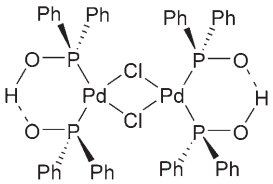

24

Figure 4. POPd dimer complex **24**.

phosphinites,[22] the crystallization of [(B-[3.2.0]DPO)PdCl$_2$] is possible in wet DCE or CHCl$_3$ and is stable to heating at 60°C over several hours. Nevertheless, **24** was tested as a catalyst/procatalyst for the cycloisomerisation of **1**→**2a–c** (Table 4).

In the presence of catalytic quantities of **24** little cycloisomerisation activity was seen (entry 1). Addition of 5 mol% NaBAr′$_4$ promoted cycloisomerisation, producing products **2a–c** (entry 2). The result highlights the importance of the ligand backbone. Furthermore, we were able to evaluate the neutral and cationic Pd(II) complexes **25** and **26** containing two monophosphinite ligands (Figure 5). Whilst complex **25** exhibits no cycloisomerisation activity, complex **26**, formed *in situ* by reaction of **25** with NaBAr′$_4$, isomerizes **1** to **1′** only.

We went on to investigate modifications to the backbone structure of the bicyclic skeleton. Novel ligand **28** was prepared from the known diol compound **27**[14] in 85% yield using standard conditions (Scheme 4). This ligand reacts quantitatively with (CH$_3$CN)$_2$PdCl$_2$ in CH$_2$Cl$_2$ to give complex **29**. Complex **29** in CDCl$_3$ solution exhibits a pair of doublets (P1 at $\delta = 103.67$, P2 at $\delta = 106.83$, $\Delta\delta_{PP} = 3.16$); a lower difference in chemical shift for the two phosphorus environments compared to [(B-[3.2.0]DPO)PdCl$_2$] (P1 at $\delta = 100.12$, P2 at $\delta = 106.33$, $\Delta\delta_{PP} = 6.21$). A large $^2J_{PP}$ spin-spin coupling (56.6 Hz) was observed, derived from *cis*-coordination of the ligand to Pd(II), which is higher than [(B-[3.2.0]DPO)PdCl$_2$] ($^2J_{PP} = 51.1$ Hz). Complex **29** crystallised from CDCl$_3$, which allowed the X-ray crystal structure to be determined (Scheme 4). Interestingly, there is a difference in the bite angle in **29** when compared with [(B[3.2.0]DPO)PdCl$_2$] {for **29**, P1–Pd–P2 = 94.01(2)°; for [(B[3.2.0]DPO)PdCl$_2$], P1–Pd–P2 = 95.99(2)°}.[14]

Table 4. Catalytic activity of POPd dimer complex **24** in the cycloisomerisation of **1**.[a]

Entry	Additive	**1**	**2a**	**2b**	**2c**
1	-	>99	-	-	-
2	$NaBAr'_4$[b]	15	26	31	15

[a] *Reagents and conditions:* identical to Table 1.
[b] Isomerised **1′** (13%) detected.

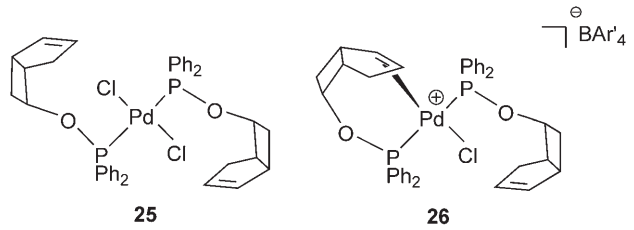

Figure 5. Monophosphinites containing the bicyclo[3.2.0]-heptane ring.

Complex **29** in the presence of $NaBAr'_4$ mediates 1,6-diene cycloisomerisation in DCE at 60 °C, albeit slowly. After 4 h, the conversion to **2b** was 10% (**2a** and **2c** not observed). After 24 h, the conversion rises to 43%, with the isomer selectivity remaining >99%. To summarise this section, a very subtle modification to the ligand structure has a pronounced effect on the rate of the cycloisomerisation reaction; other modifications in the bicyclic structure would similarly be expected to exert dramatic effects on the reaction rate and potentially product selectivity.

Solution and Solid-State Behaviour of the Cationic Pd(II) Phosphinite Complexes

To gain an insight into the solution behaviour of the monocationic complexes [(B[3.2.0]DPO)Pd-(solv)Cl]$^+$[X]$^-$ (**4a–d**), ^{31}P NMR spectroscopic studies were carried out. Firstly, to a $CDCl_3$ solution of [(B-[3.2.0]DPO)$PdCl_2$] was added $AgBF_4$ (1 equiv.) at 25 °C (c = 100 mM);[23] the ^{31}P NMR spectrum of this reaction exhibited two broad signals (Figure 6).

At −20 °C these peaks sharpen to give two strong doublets (P1 at δ = 105.90, P2 at δ = 99.01, $\Delta\delta_{PP}$ = 6.89, $^2J_{PP}$ = 49.7 Hz). At −50 °C, another minor species becomes resolved (P1 at δ = 103.37; P2 at δ = 91.28, $\Delta\delta_{PP}$ = 12.09, $^2J_{PP}$ = 55.7 Hz). Given the absence of a donor solvent (e.g., acetonitrile or methanol), and the small difference in chemical shift, the major species appears to be the Pd(II) dimer complex **30a** with two bridging chlorides, which is in equilibrium with the monomeric complex **4a**. To confirm this hypothesis an identical experiment was performed in a mixture of $CDCl_3/CD_3CN$ (4:1, *v/v*) (Figure 7). The ^{31}P NMR spectra of [(B[3.2.0]DPO)$PdCl_2$] in $CDCl_3$ (spectrum A) and in $CDCl_3/CD_3CN$ (spectrum B) are shown for comparison (a small solvent-induced shift, *ca.* 1 ppm, is seen in spectrum B). On addition of $AgBF_4$ (1 equiv.) to this solution, two new species are formed at δ = 103.98 and δ = 91.88, appearing as doublets ($\Delta\delta_{PP}$ = 12.1; $^2J_{PP}$ = 54.4 Hz) (spectrum C). The similar chemical shift and spin-spin coupling constant of the minor species observed at −50 °C in Figure 6, confirms that this is most likely the monomeric complex [(B[3.2.0]DPO)Pd(CD_3CN)Cl]$^+$[BF_4]$^-$ **4a**. The obser-

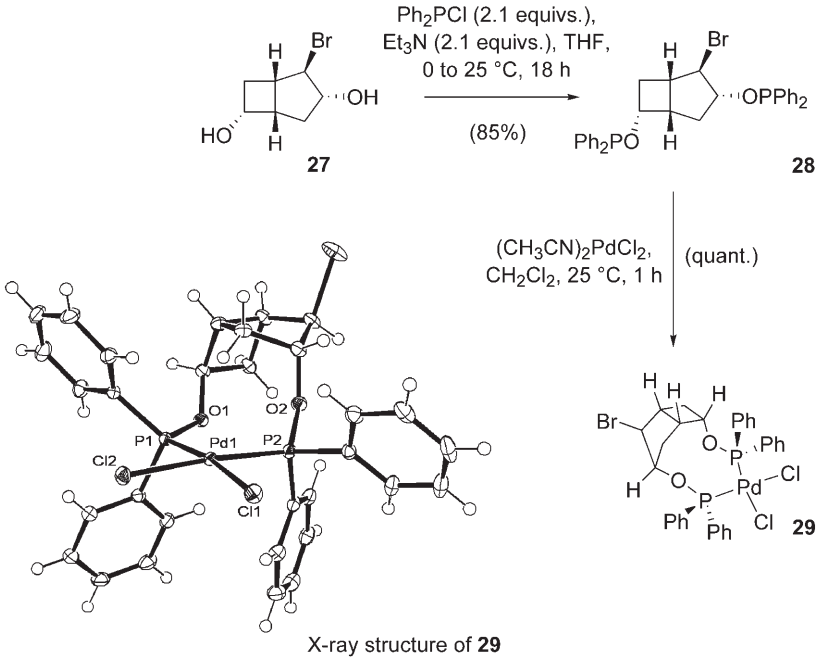

Scheme 4. Synthesis of a brominated variant of [(B[3.2.0]DPO)$PdCl_2$].

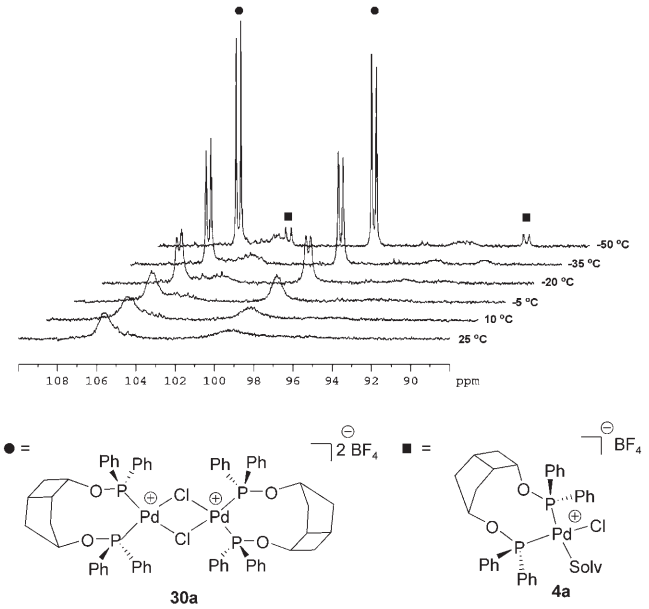

Figure 6. Variable temperature ^{31}P NMR spectra of [(B-[3.2.0]DPO)PdCl$_2$]/AgBF$_4$ (1:1) in CDCl$_3$ (202 MHz, in CDCl$_3$); solv. = CDCl$_3$ or H$_2$O (reversible on re-warming the solution).

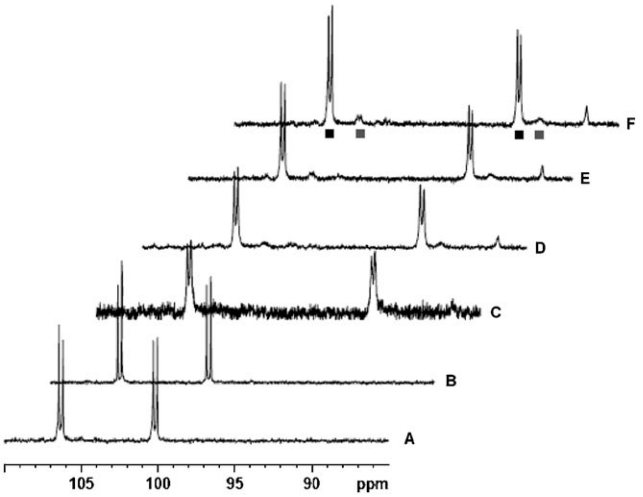

Figure 7. ^{31}P NMR spectra of [(B[3.2.0]DPO)PdCl$_2$]/AgBF$_4$ (1:1) (c = 12 mM, 202 MHz): spectrum A = [(B-[3.2.0]DPO)PdCl$_2$] in CDCl$_3$; spectrum B = [(B-[3.2.0]DPO)PdCl$_2$] in CDCl$_3$/CD$_3$CN (4:1, *v/v*); spectrum C = [(B[3.2.0]DPO)PdCl$_2$]/AgBF$_4$ (1:1) at 25 °C; spectrum D = [(B[3.2.0]DPO)PdCl$_2$]/AgBF$_4$ (1:1) at −5 °C; spectrum E = as for D, at −20 °C; spectrum F = as for E, at −35 °C. Key: ■ major monomeric species **4a**; ■ minor monomeric species **4a′**.

vation of a minor species at δ = 102.1 and δ = 90.3 ($\Delta\delta_{PP}$ = 11.8; unresolved) is likely to be the isomeric form of the major complex species (see later for discussion).

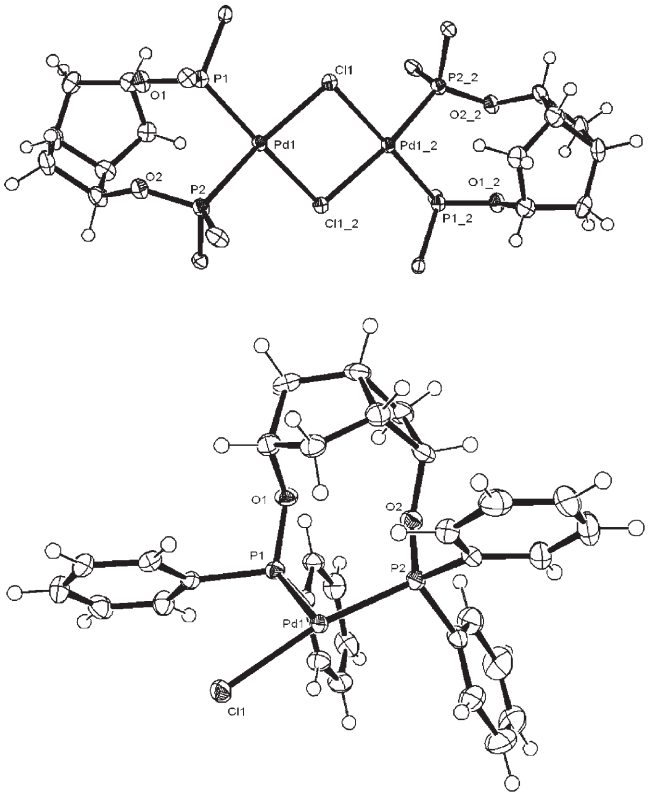

Figure 8. X-ray crystal structure of **30b**. Top: complex with phenyl groups on phosphorus removed, and 2 × OTf and 2 × CHCl$_3$ omitted for clarity. Bottom: Asymmetric unit with OTf and CHCl$_3$ omitted for clarity. Thermal ellipsoids at 50% probability level. Bond angles (°): O(1)–P(1)–Pd 119.58(11), O(2)–P(2)–Pd 115.55(11), P(1)–Pd–Cl(1) 93.81(3), P(2)–Pd–Cl(1) 169.60(4), P(2)–Pd–P(1) 90.10(4); Bond lengths (Å): O(1)–P(1) 1.587(3), O(2)–P(2) 1.581(3), P(1)–Pd 2.259(10), P(2)–Pd 2.232(10), Pd–Cl(1) 2.410(9), Pd–Cl(1) 2.393(10).

In CDCl$_3$, in the presence and absence of acetonitrile, similar spectra were seen for the reaction of [(B-[3.2.0]DPO)PdCl$_2$] with AgOTf (1 equiv.). From the CDCl$_3$ solution crystallised the dicationic Pd(II) dimer complex **30b**, after several weeks at 25 °C in the absence of acetonitrile (Figure 8).[24] The key bond angles and bond lengths are given in Figure 8, however note that a narrow P–M–P′ bite angle is observed (90.1°), which is significantly different to the bite angle found in [(B[3.2.0]DPO)PdCl$_2$] (95.9°).[14] Crystals of **30b** dissolve in CDCl$_3$, giving rise to two broad phosphorus signals at δ = 98.88 and δ = 105.78; the chemical shifts confirm that this is a dimer in CDCl$_3$ solution.

The ^{31}P NMR spectra from the reaction of [(B-[3.2.0]DPO)PdCl$_2$] with NaBAr′$_4$ (1 equiv.) in CDCl$_3$ alone were complex. At low temperature, several species were observed. Superior spectra were obtained from the reaction of [(B[3.2.0]DPO)PdCl$_2$] with NaBAr′$_4$ (1 equiv.) in CDCl$_3$/CD$_3$CN (4:1, *v/v*)

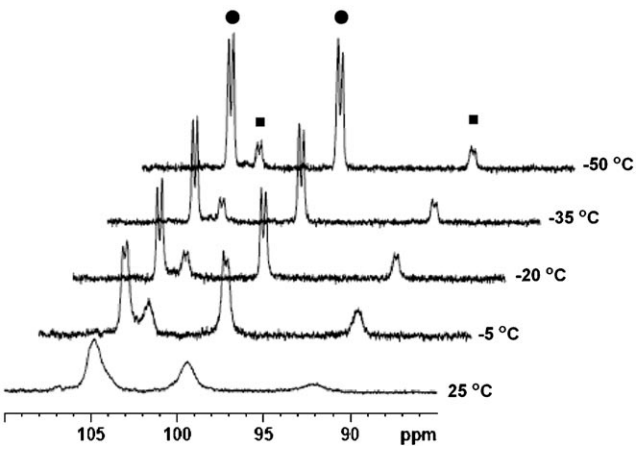

Figure 9. Variable temperature ^{31}P NMR spectra of [(B-[3.2.0]DPO)PdCl$_2$]/NaBAr′$_4$ (1:1) in CDCl$_3$/CD$_3$CN (4:1) (c = 12 mM, 202 MHz). Key: ● dimeric species **30d**; ■ monomeric species **4d**.

(Figure 9). At 25 °C, two pairs of broad signals were observed; a major species at δ = 104.1 and δ = 99.3 and minor species at δ = 103.7 (overlapping with δ = 104.1) and δ = 92.3 (Figure 9). The major species cleanly resolves to give a pair of doublets at lower temperatures ($^2J_{PP}$ = 54.5 Hz at −50 °C). The minor species resolves to a certain extent, although not cleanly, the chemical shifts of which point to this being [(B[3.2.0]DPO)Pd(solv)Cl]$^+$[BAr′$_4$]$^-$ **4d** (the only isomer detected). Halving the concentration results in complex **4d** becoming the major species in solution. Attempts to crystallise the monocationic complexes [(B[3.2.0]DPO)Pd(solv)Cl]$^+$[X]$^-$ (solv = CH$_3$CN, MeOH or CHCl$_3$, X = BF$_4$, OTf or BAr′$_4$) have been unsuccessful.

From these NMR spectroscopic studies we are able conclude that coordinating anions in CDCl$_3$, e.g., BF$_4$ or OTf, favour formation of the dimeric Pd(II) complexes **30a** and **30b**. In the presence of added coordinating solvent (e.g., CD$_3$CN), the monomeric Pd(II) complexes **4a** and **4b** are observed exclusively, even at 25 °C. At lower temperature the major and minor isomers of the monomeric species are detected. The situation is different for non-coordinating anions (e.g., BAr′$_4$); in CDCl$_3$ a dynamic process is apparent, which on cooling revealed a large number of different species. On addition of CD$_3$CN, a rapid equilibrium between dimeric and monomeric Pd(II) species was observed, which on cooling showed the predominant appearance of the dimeric Pd(II) species **30d**, as well as the major isomer of the monomeric Pd(II) complex **4d**. The proposed equilibrium is depicted in Scheme 5; the isomeric forms are shown as **4** and **4′**.

On the Conformation of the Bicyclic Ring

Although the variable temperature ^{31}P NMR experiments did not reveal different conformers in solution at low temperature, direct evidence for the existence of the higher energy *exo*-envelope conformation in the bicyclo[3.2.0]heptane skeleton was revealed in the formation of a unique Pd(0) dimeric complex [Pd$_2$(B-[3.2.0]DPO)$_3$], containing three bridging B[3.2.0]DPO ligands, prepared by reaction of Pd$_2$(dba)$_3$ with excess B[3.2.0]DPO (*ca.* 3 equivs. per Pd), which was characterized principally by X-ray diffraction studies (Figure 10).[25] Overall, this establishes that the ligand can adopt both *endo* and *exo*-envelope conformations.

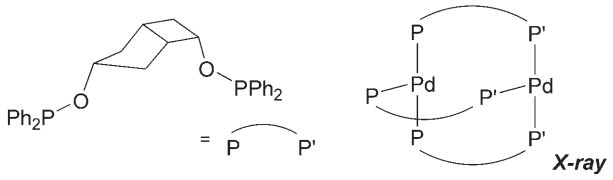

Figure 10. First example of B[3.2.0]DPO showing an *exo*-envelope conformation.

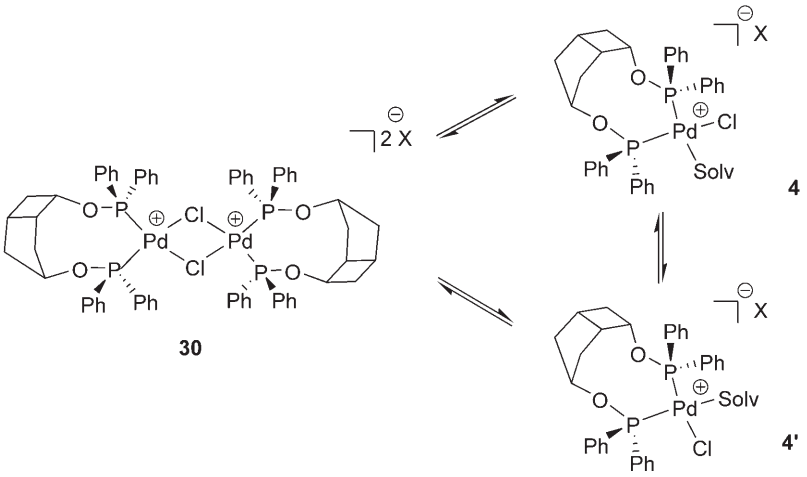

Scheme 5.

Theoretical Studies

The dynamic behaviour of the monocationic complexes in solution, and the identification of the *exo*-envelope conformation in $[Pd_2(B[3.2.0]DPO)_3]$ in the solid-state, led us to consider further the potential for conformational change in the bicyclic backbone. With the results provided above and given that such ring-flips are well documented for the bicyclo-[3.2.0]heptane ring system, this is conceivable.[26] The equilibria are complicated by the ligand containing two phosphinite environments in the cyclobutyl and cyclopentyl rings, which means that the chloride ligand may be *cis* or *trans* with respect to the C3 and C6 phosphinite groups leading to the two different isomeric forms. The relative stability of the proposed structures (**I** and **II**) shown in Scheme 6 were thus studied. Several structural isomers for the model cationic complex $[\{Me_2PO(bicycloheptyl)OPMe_2\}PdCl]^+$ were calculated (optimised) with the aid of density functional theory calculations at the B3LYP level.

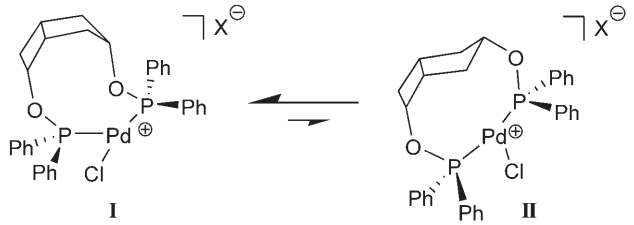

Scheme 6. The *endo*-to-*exo* envelope ring-flip.

Three relevant structural isomers were obtained from these calculations. Isomer **A3** adopts a square planar geometry around Pd and possesses an agostic bond with an *endo*-disposed cyclopentyl hydrogen atom (Figure 11). The conformation of the bicycloheptyl moiety in this isomer is similar to that in **II**. The relative energies indicate that **A3** is unstable, although containing an additional agostic bond. Structure **A3** shows longer P–O and Pd–P bonds in comparison with **A1** and **A2** (Figure 12). Therefore, the instability of **A3** is likely due to the structure experiencing strain as a result of maintaining favourable Pd–P bonding interactions. Both **A1** and **A2** adopt a T-shaped geometry around Pd, as expected for 14-electron ML_3 complexes. The stability of the two structural isomers is similar to each other. **A1** is more stable than **A2** by 3.2 kcal mol^{-1}. On examining the structures of **A1** and **A2**, we believe that in **A1** the repulsive interactions between the chloro ligand and the two R groups associated with the phosphorus atom *cis* to it are smaller than the corresponding repulsive interactions in **A2**. In each of the two isomers, there are two 1,4-repulsive interactions between Cl and the two R groups associated with the phosphorus atom *cis* to it. In the T-shaped **A1** structure, the smaller Cl–Pd–P–Me dihedral angle is 49.4°, while in **A2** the smaller Cl–Pd–P–Me dihedral angle is 20.2°.

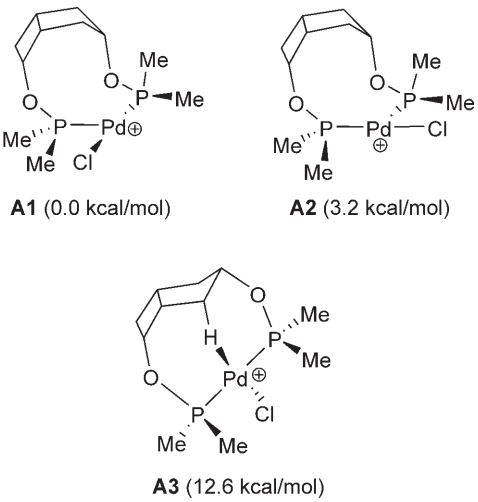

Figure 11. Relative energies of the monocationic Pd(II) complexes.

Based on the relative energies calculated for the three structural isomers, we believe that the major and minor species observed on cooling a $CDCl_3$ solution of the mono-cationic complexes **4a–d** should be related to the **A1** and **A2** structures, respectively. The **A3** structure is too high in energy to be in equilibrium with other structural isomers at temperatures below 0 °C (Scheme 7).

The exchange between the chloro ligand and the coordinated solvent ligand is expected to be a slow process, allowing the detection of the two species in solution at low temperature. The reason to propose an equilibrium involving the solvent is as follows. The complexity in the structure of the diphosphinite ligand should give rise to some other energy minimum structures. However, we do not expect larger barriers for the interchange processes among these energy minimum structures. In other words, we expect a fluxional nature of the diphosphinite ligand in solution. The observation of more than one species in solution from the ^{31}P NMR spectra is unlikely due to the different conformers adopted by the diphosphinite ligand (due to high energy of **A3**, 12.6 kcal mol^{-1}).

Interestingly, when Cl is replaced with H, we found that the **A3_H** structure is the most stable (Figure 12). The energy difference between **A1_H** and **A2_H** is smaller than that between **A1** and **A2**. A hydride ligand is small and creates smaller repulsive interactions when compared with a chloro ligand, giving smaller energy difference between the two structures. The high stability of the **A3_H** structure can be related to the strong *trans*-influencing property

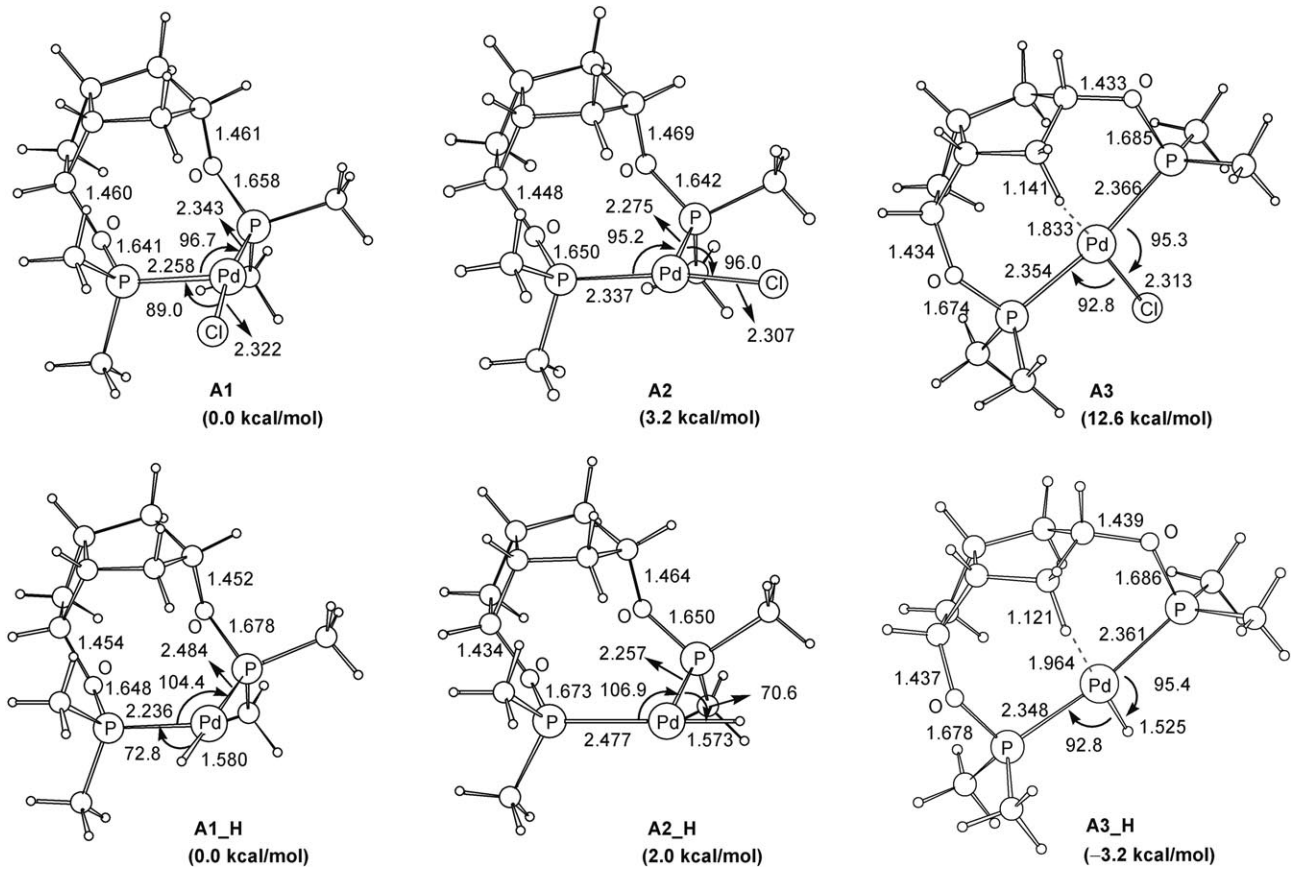

Figure 12. Calculated structures for the model complexes $[\{Me_2PO(bicycloheptyl)OPMe_2\}PdCl]^+$ and $[\{Me_2PO(bicycloheptyl)OPMe_2\}PdH]^+$. The bond distances are given in angstroms and the bond angles in degrees (agostic interaction shown in broken lines).

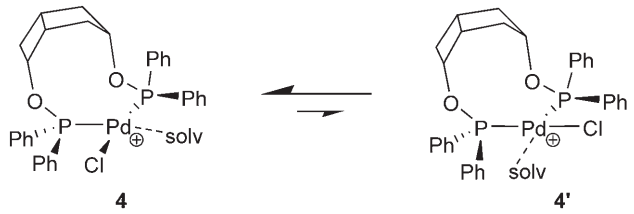

Scheme 7. Equilibrium between **4** and **4′**.

of the hydride ligand. The strong *trans*-influencing hydride ligand destabilises both the **A1_H** and **A2_H** structures because it significantly weakens the Pd–P bond *trans* to it (Figure 12). In each of the **A1 H** and **A2_H** structures, the Pd–P bond *trans* to the hydride ligand is longer than the other Pd–P bond by more than 0.22 Å. In the **A3_H** structure, the hydride ligand is *trans* to the agostic bond and has the shortest distance with the metal centre in the three structures. Despite the high stability of the **A3_H** structure, we do not expect that it is the major species in the solution because the other two less stable structures should have greater solvation energies due to their coordination unsaturation. However, contrary to what we see for the chloro complex, we expect that the population of the **A3_H** structure in solution, due to its high intrinsic stability, should be comparable to the other two species, making the **A3_H** structure potentially observable in solution. At higher temperatures, e.g., 60 °C, one may confidently predict that the **A3/A3_H** conformer could play a role in catalysis.

On the Ligand Effects and Mechanistic Discussion

Monocationic Pd(II) complexes **4a–d**, containing a B-[3.2.0]DPO ligand, promote the catalytic cycloisomerisation of **1** to give **2a–c**. The regioselectivity is influenced on changing the anion on Pd(II) (e.g., BAr'_4, BF_4, OTf and SbF_6), with the best selectivity found for the more bulky and non-coordinating BAr'_4 anion. It was determined that the neutral complex was an ineffective cycloisomerisation catalyst/procatalyst. In contrast, the dicationic complexes, although more active in cycloisomerisation, resulted in lower isomer selectivity. A screen of other diphosphine and diphos-

phinite ligands has revealed that B[3.2.0]DPO is a unique ligand for cycloisomerisation. It was possible to eliminate other possibilities as the active catalyst species through testing the POPd dimer complex **24** in the presence and absence of $NaBAr'_4$, which showed poor isomer selectivity in comparison with **4d**. Removal of the C3 phosphinite, as in Pd(II) complex **25**, again resulted in poor isomer selectivity. Interestingly, modification of the ligand backbone to include a C2 *exo*-bromo substituent (e.g., in **30**) exhibited lesser catalytic activity compared to **4a** and **4d**.

^{31}NMR spectroscopy clearly indicates that complexes **4a–d** are in equilibrium with the dimeric complexes **30a–d**. On the other hand, the DFT calculations and solid-state studies support the proposal that the B[3.2.0]DPO ligands are flexible enough to allow changes in bite angle. The question that needs to be addressed is whether this structural property is important for the 1,6-diene cycloisomerisation process. On a general note, ligand bite angles can influence catalytic activity in transition metal catalysed processes considerably. Indeed, Van Leuween and co-workers have elegantly demonstrated that substantial changes in rates and selectivities are seen in hydroformylation, hydrocyanation, allylic alkylation and cross-coupling reactions as a function of altering the ligand bite angle.[27] Relevant to our investigations are the studies reported by DuBois and co-workers who have shown that the ligand bite angle is able to control the hydricity of Pd(II) diphosphine complexes.[28] For a series of $[Pd(diphosphine)_2][BF_4]_2$ and $[Pd(diphosphine)_2]$ complexes, it was established that Pd(II) complexes with small bite angles exhibit a geometry that is very close to square planar, while ligands with large bite angles distort the geometry from square planar to near tetrahedral. Such a distortion towards a tetrahedral geometry results in stabilisation of the LUMO, resulting in a more favourable formation of a Pd(II) hydride species. Consequently, Pd(II) diphosphine complexes with large bite angles are good hydride acceptors and poor hydride donors and, *vice versa*, we can predict that complexes with smaller bite angles are more likely to donate their hydride. Any variation in the natural bite angle of the ligand will alter the hydricity of the Pd(II) hydride. Although their study focused on phosphines and not phosphinites, we may propose that monocationic Pd(II) complexes **4a–d** can flip between two conformational forms, allowing at least two bite angles. In the *exo*-envelope the Pd(II) hydride species is stabilised, while a flip to the *endo*-envelope would facilitate hydride donation. Since the reactions are at elevated temperatures (60 °C) we would expect that there is a higher population of the *exo*-conformer of the ligand, enabling stabilisation of the Pd(II) hydride.

Consideration of the ligand coordination and the bite angles exerted by B[3.2.0]DPO goes some way to explaining the poor reactivity of the other bidentate phosphine and phosphinite ligands **7–10**. Simple molecular models of the Pd(II) complexes containing these ligands indicate relatively small ligand bite angles *ca.* 90–100°, which are less flexible than B-[3.2.0]DPO. A small bite angle would lead to the subsequent monocationic Pd(II) complex being less likely to form the Pd(II) hydride species resulting in poor catalytic activity.

The reaction kinetics showed pseudo first-order behaviour in **1**, which stands in contrast to the pseudo zero-order behaviour established for different Pd(II) catalyst systems by other groups.[6b,29] Given the comprehensive experimental evidence supporting the involvement of a Pd(II) hydride as the active catalyst species,[32] the unexpected outcome in the reaction order with respect to **1** allows us to propose $[(B\text{-}[3.2.0]DPO)PdH]^+[X]^-$ as being the catalyst resting state, which is ultimately regenerated in each turnover, and moreover dependent on the concentration of **1**. To probe the involvement of a Pd(II) hydride species, $Pd_2(dba)_3$ was reacted with B[3.2.0]DPO (Pd:L, 1:1) in DCE at 25 °C to give the intermediate $[(BC[3.2.0]DPO)Pd(0)(\eta^2\text{-dba})]$ {P1 at $\delta = 108.1$ and P2 at $\delta = 109.8$ (br s), $\Delta\nu_{1/2} = 40$ Hz }, which is not an active cycloisomerisation catalyst in its own right. A solution of HBF_4 (54 % in Et_2O, 1 equiv. with respect to Pd) was added to this to generate initially $[(BC\text{-}[3.2.0]DPO)Pd(0)(\eta^2\text{-dba-}H^+)][BF_4]^-$ {P1 at $\delta = 108.9$ and P2 at $\delta = 109.2$ (br s); $\Delta\nu_{1/2} = 18$ Hz}, which degrades to give a new species appearing as a pair of doublets {P1 at $\delta = 105.8$ and P2 at $\delta = 110.4$; $^2J_{PP} = 52.5$ Hz). This species is most likely $[(B\text{-}[3.2.0]DPO)Pd(solv)H]^+[BF_4]^-$. Addition of **1** (20 equivs.) to this solution resulted in some cycloisomerisation (ratio of **1′**:**2b**:**2c**, 32:7:35), and although this outcome does not mirror the reaction mediated by the $[(B[3.2.0]DPO)PdCl_2]/AgBF_4$ catalyst system (entry 4, Table 1), it indicates that cycloisomerisation of **1**→**2b** and **2c** is possible, as is the isomerisation **1**→**1′**.[30]

Our proposed mechanism for 1,6-diene cycloisomerisation (Scheme 8) is similar to the Widenhoefer mechanism [with cationic palladium(II) phenanthroline complexes],[31] and Lloyd-Jones mechanism [with neutral palladium(II) complexes containing nitrile ligands],[6b] and supported by our experimental findings (Scheme 6). The catalytic cycle is dependent on the generation of $[(B[3.2.0]DPO)PdH]^+$ (**II**) from $[(B\text{-}[3.2.0]DPO)PdCl]^+$ (**I**); it is currently not clear how this occurs. The phosphinite ligand could undergo a series of associative/dissociative processes (bidentate→monodentate) throughout the catalytic cycle (not shown for simplicity). Hydropalladation of a tethered alkene in **1** would form palladium alkyl

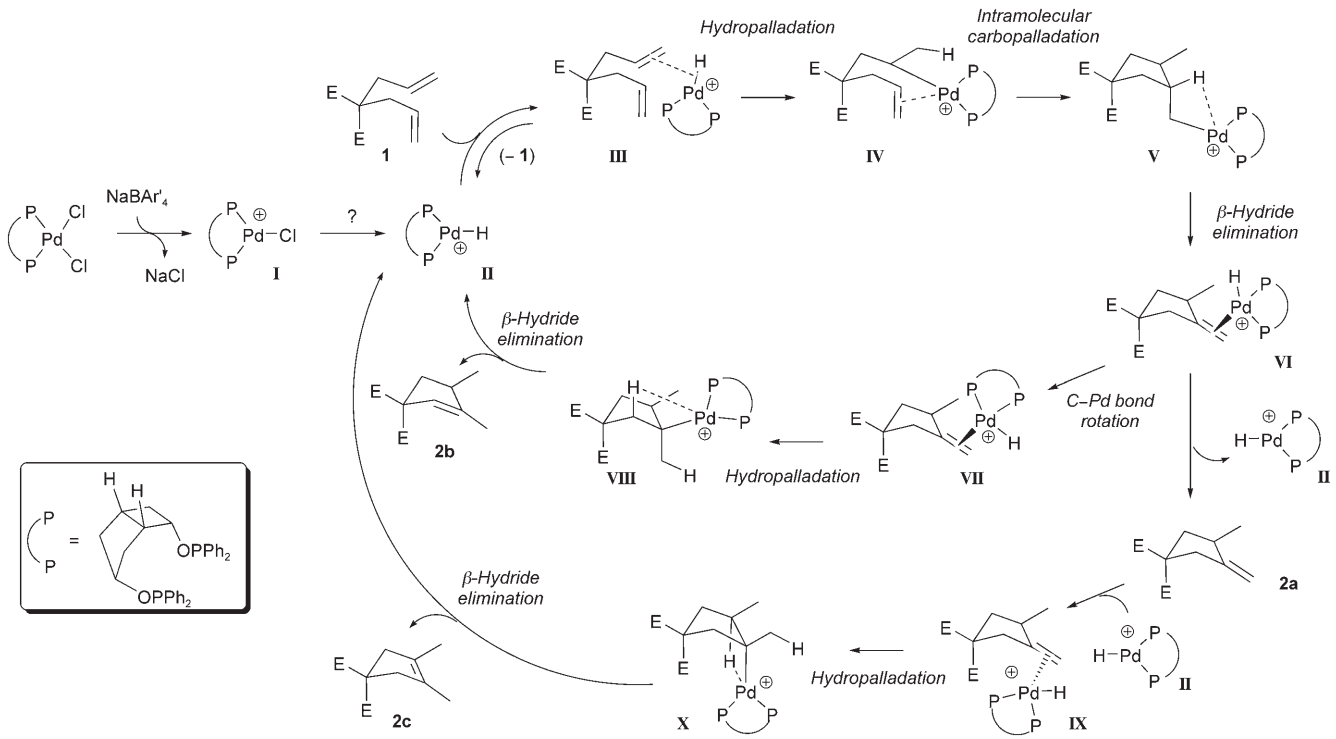

Scheme 8. Plausible mechanism for cycloisomerisation of 1,6-dienes mediated by cationic Pd(II) complexes containing B-[3.2.0]DPO ligands.

alkene intermediate **IV**, *via* initial intermediate **III**. The reaction kinetics suggest that this step is slow. The pseudo first-order behaviour is consistent with the intermolecular capture of the Pd–H/insertion step. Monodentate coordination of the 1,6-diene **1** is presumably reversible, with the pseudo first-order arising from the dependence of this equilibrium on the concentration of **1**. Intramolecular carbopalladation of **IV** reveals palladium cyclopentylmethyl complex **V** which then undergoes β-hydride elimination to form palladium methylenecyclopentane complex **VI**. Loss of **II** provides product **2a**. A second hydropalladation event in **VII** provides the *syn* tertiary palladium cyclopentylmethyl complex **VIII**, from which a regioselective β-hydride elimination process from the secondary hydrogen atom in **VIII** forms product **2b**, regenerating $[(B[3.2.0]DPO)PdH]^+$ (**II**). Note that β-hydride elimination cannot occur from the more substituted carbon in **VIII**.[6b] The formation of **2c** can be rationalised through steps **IX**→**X**. Recoordination of **II** to **2a** gives alkenyl Pd(II) complex **IX**. Hydropalladation *anti* to the β-methyl substituent gives *anti* tertiary palladium cyclopentylmethyl complex **VIII** and subsequent *syn* β-hydride elimination, which can then undergo a *syn* β-hydride elimination to reveal **2c** with regeneration of **II**.

The finding that $[(B[3.2.0]DPO)PdCl]^+[BAr'_4]^-$ rapidly isomerizes **2a** to both **2b** and **2c**, provides support for this mechanism. The formation of **2b** through this pathway indicates that the Pd(II) hydride moiety does not dissociate prior to the second hydropalladation event (**VI**→**VII**→**VIII**). The very slow isomerisation of **2b** to **2c** indicates that **2b** is also a poor ligand for **II**, whereas **2a** is an excellent ligand.

Conclusions

In summary, a regioselective catalyst for 1,6-diene cycloisomerisation has been identified. B[3.2.0]DPO is clearly an exceptional ligand for this process, providing that a non-coordinating anion is using in combination with Pd(II). In due course, our findings regarding the asymmetric process will be reported.

Experimental Section

General Remarks

Solvents were dried where necessary using standard procedures prior to use and stored under an argon atmosphere. Nitrogen gas was oxygen-free and was dried immediately prior to use by passage through an 80 cm column containing sodium hydroxide pellets and silica. Argon gas was used directly *via* balloon transfer or on a Schlenk line. TLC analysis was performed routinely using Merck 5554 aluminium-

backed silica plates or Macherey–Nagel polygram® ALOX N/UV254 aluminium oxide-coated plastic sheets. Compounds were visualised using UV light (254 nm) and a basic aqueous solution of potassium permanganate or acidic DNP (dinitrophenol hydrazine). GC parameters: analysis was performed using a Varian CP-3800 GC equipped with a CP-8400 Autosampler. Separation was achieved using a DB-1 column (30 m × 0.32 mm, 0.25 μm film thickness) with carrier gas flow rate of 3 mL min^{-1} and a temperature ramp from 50 °C to 250 °C at 20 °C min^{-1}. The injection volume was 1 μL with a split ratio of 50. Mass spectrometry was carried out using a Fisons Analytical (VG) Autospec instrument. ^{1}H NMR spectra were recorded at 400 MHz using a JEOL ECX 400 spectrometer or 500 MHz on a Bruker AV 500 spectrometer; ^{31}P NMR spectra were recorded at 202 MHz (^{1}H decoupled). Chemical shifts are reported in parts per million (δ) downfield from an internal tetramethylsilane reference. Coupling constants (*J* values) are reported in Hertz (Hz), and spin multiplicities are indicated by the following symbols: s (singlet), d (doublet), t (triplet), q (quartet), m (multiplet), br (broad).

Compounds **1** (prepared from dimethyl allylmalonate), **2a–c**, **14–20** and **22** have been previously reported (the NMR and MS data are in agreement with literature data).[6b,d] Complexes **24--26** have been reported previously.[14] NaBAr′$_4$ was prepared as described by Brookhart et al.,[32a] taking into consideration the points made by Bergmann and Yakelis.[33b] $AgBF_4$, AfOTf, $AgSb_6$ and anhydrous DCE were purchased from Sigma–Aldrich. Reagent grade DCE was purchased from Alfa-Aesar.

General Procedure for 1,6-Diene Cycloisomerisation

To a stirred solution of the 1,6-diene (50 mg, 0.236 mmol, 1 equiv.) in analytical reagent grade DCE (1 mL) was added [(B[3.2.0]DPO)$PdCl_2$] (7.9 mg, 0.012 mmol, 0.05 equivs.), followed immediately by the appropriate metal counter ion (0.012 mmol, 0.05 equivs.), at room temperature. The reaction was heated in a preheated oil bath at the relevant temperature (temperature quoted is that of the oil-bath and monitored by an external temperature probe, ±1 °C). An aliquot from each reaction mixture (*ca.* 30–50 μL) was filtered through a short silica-gel plug using CH_2Cl_2 (1 mL), which was concentrated under vacuum (no further conversion was detected in these analysis samples). This sample was taken up in $CDCl_3$ and reaction progress monitored by ^{1}H NMR spectroscopy. On several occasions GC was employed to monitor reaction progress. Conversions by GC were compared with those determined by ^{1}H NMR spectroscopy, through integration of the methyl signals of the cycloisomerisation products or the methylene signals of the 1,6-diene.

Synthesis of Ligand 28

Under an atmosphere of argon a THF solution (10 mL) of diol **27**[14] (400.0 mg, 1.9 mmol, 1 equiv.) was cooled to 0 °C and then Et_3N (562 μL, 4.04 mmol, 2.1 equivs.) in THF (2 mL) was added by cannula and allowed to stir at this temperature for 0.5 h. Chlorodiphenylphosphine (740 μL, 4.04 mmol, 2.1 equivs.) was added dropwise slowly at 0 °C. $Et_3N{\cdot}HCl$ formed immediately (precipitate). The mixture was allowed to warm to 25 °C and stirring was continued for 16 h. After this time, the mixture was passed through Celite® under nitrogen atmosphere [washed through with THF (50 mL)]. The solvent was removed under vacuum to give **28** as a viscous cloudy white oil (>85 % yield), which was reacted directly with $(CH_3CN)_2PdCl_2$ in the next step. This compound was handled as the free ligand in a dry-box, as it is air sensitive. Selected data: ^{31}P NMR (dry and degassed $CDCl_3$, 202 Hz): δ = 108.42 (s) and 114.01 (s).

[3-*endo*-6-*endo*-Bis(diphenylphosphinooxy)-2-*exo*-bromobicyclo[3.2.0]heptanyl]palladium(II) Chloride (29)

To a solution of **28** (182 mg, 0.31 mmol, 1 equiv.) in dry CH_2Cl_2 (3.0 mL) was added via cannula transfer a solution of $(CH_3CN)_2PdCl_2$ (93 mg, 0.31 mmol, 1 equiv.) in CH_2Cl_2 (3 mL). The solution was allowed to stir for 2 h at 25 °C. The solvent was removed under vacuum to afford a pale yellow solid; yield: 145 mg (70 %); mp 228–229 °C (decomp.); ^{1}H NMR ($CDCl_3$, 500 MHz): δ = 2.22 (1 H, m, H4$_{exo}$), 2.35 (2 H, m, H5 and H4$_{endo}$), 2.78 (2 H, m, H1 and H7$_{exo}$), 3.26 (1 H, d, ^{2}J = 15.6, H7$_{endo}$), 4.19 (1 H, 2, H2), 4.29 (1 H, br s, H3$_{exo}$), 4.50 (1 H, t, ^{2}J = 4.2, H6$_{exo}$), 7.28 (3 H, m, Ar), 7.53 (10 H, m, Ar), 7.75 (3 H, m, Ar), 7.98 (4 H, m, Ar); ^{31}P NMR ($CDCl_3$, 202 Hz): δ = 103.67 (d, ^{2}J = 56.6 Hz), 106.83 (d, ^{2}J = 56.6 HZ); MS (FAB): *m/z* = 717 (M^+−Cl, 66), 682 (M^+−2 Cl, 8), 573 (M^+−2 Cl-Pd, 7), 509 (17), 461 (27), 401 (60), 281 (37), 207 (45), 147 (100), 139 (95); anal. calcd. for $C_{31}H_{29}O_2P_2Cl_2BrPd$: C 48.46, H 3.88; found: C 48.74, H 4.04.

General Procedure for the Monocationic Pd(II) Complexes

Detailed information concerning the characterisation of these complexes can be found in the main text of the paper.

With magnetic stirring, a $CDCl_3$ solution (0.5 mL), or $CDCl_3/CD_3CN$ solution (4:1, *v/v*), containing [(B-[3.2.0]DPO)$PdCl_2$] (10 mg, 1.5×10^{-5} mol) was added the appropriate metal salt (1.5×10^{-5} mol). A precipitate forms almost immediately. The solid precipitate was allowed to settle, and then the solution was transferred by cannula to a NMR tube, and analysed directly by NMR spectroscopy. The solutions were injected into an ESI-MS/MS to confirm the molecular ions (in + mode) and anions (in − mode); MS (ESI, + mode): *m/z* = 636.9 (M^+−BAr′$_4$, 100); identical spectra were obtained for the dimer (doubly charged) and monomer (singly charged) complexes.

Variable Temperature ^{31}P{^{1}H} NMR Experiments

Experiments were run on a Bruker AV 500 spectrometer, running at 202.47 MHz. Where a mixture of $CDCl_3/CD_3CN$ was used, the solvent lock was on $CDCl_3$. A low temperature calibration was performed using neat MeOH as previously described.[33] In brief, with the sweep set to off, a ^{1}H NMR spectrum was recorded. The difference between the two proton signals (A and B) represents an absolute value of Δν in Hz at a given temperature. Using the following equation, with the appropriate values of A and B, the actual temperature of the sample was calculated {$T_{calibrated}$ (K) = 403 − A·Δν − B·(Δν)^2} (A = 0.059 and B = 9.53×10^{-5} at 500 MHz).

Computational Details

Density functional theory calculations at the B3LYP level were performed to calculate the structures of the model complexes.[34] The effective core potentials (ECPs) of Hay and Wadt with a double-ζ valance basis set (LanL2DZ) were used for Pd, Cl, and P.[35] The 6–31G basis set was used for C, H, and O.[36] Polarization functions were also added for C ($\zeta_d=0.6$), O ($\zeta_d=1.154$), Cl ($\zeta_d=0.514$), and P ($\zeta_d=0.34$), and for H ($\zeta_p=1.1$) that is directly bonded to the metal centre in the metal hydride complex. All calculations were performed with the Gaussian 03 software package.[37]

Acknowledgements

I. J. S. F. thanks the Royal Society for a University Research Fellowship and generous equipment grant. We thank EPSRC for a Ph.D. studentship to S.G., Stylacats Ltd. for CASE funding, and Prof. S. M. Roberts for supporting this project. Heather Fish is thanked for assistance with low temperature NMR experiments, and Mr. B. E. Moulton for help with X-ray crystallography. We thank the University of Bologna (Italy) for supporting a research stay in York for S.T. We are grateful to Prof. G. C. Lloyd-Jones (Bristol) for discussions concerning this work.

References

[1] a) C. Aubert, O. Buisine, M. Malacria, *Chem. Rev.* **2002**, *102*, 813; b) R. A. Widenhoefer, *Acc. Chem. Res.* **2002**, *35*, 905; c) G. C. Lloyd-Jones, *Org. Biomol. Chem.* **2003**, *1*, 215.

[2] a) S. Okamoto, T. Livinghouse, *J. Am. Chem. Soc.* **2000**, *122*, 1223; b) S. Okamoto, T. Livinghouse, *Organometallics* **2000**, *19*, 1449.

[3] a) R. Grigg, J. F. Malone, T. R. B. Mitchell, A. Ramasubbu, R. M. Scott, *J. Chem. Soc., Perkin Trans.* 1 **1984**, 1745; b) A. Bright, J. F. Malone, J. K. Nicholson, J. Powell, B. L. Shaw, *Chem. Commun.* **1971**, 712.

[4] a) Y. Yamamoto, Y. Nakagai, N. Ohkoshi, K. Itoh, *J. Am. Chem. Soc.* **2001**, *123*, 6372; b) I. Özdemir, E. Çetinkaya, B. Çetinkaya, M. Çiçek, D. Sémeril, C. Bruneau, P. H. Dixneuf, *Eur. J. Inorg. Chem.* **2004**, 418; c) Y. Terada, M. Arisawa, A. Nishida, *Angew. Chem. Int. Ed.* **2004**, *43*, 4063; d) Y. Miyaki, T. Onishi, S. Ogoshi, H. Kurosawa, *J. Organomet. Chem.* **2000**, *616*, 135; e) M. Michaut, M. Santelli, J.-L. Parrain, *Tetrahedron Lett.* **2003**, *44*, 2157; f) A. Fürstner, M. Liebl, C. W. Lehmann, M. Picquet, R. Kunz, C. Bruneau, D. Touchard, P. H. Dixneuf, *Chem. Eur. J.* **2000**, *6*, 1847; g) M. Bassetti, F. Centola, D. Sémeril, C. Bruneau, P. H. Dixneuf, *Organometallics* **2003**, *22*, 4459; h) B. Çetinkaya, S. Demir, I. Özdemir, L. Toupet, D. Sémeril, C. Bruneau, P. H. Dixneuf, *Chem. Eur. J.* **2003**, *9*, 2323; i) Y. Yamamoto, N. Ohkoshi, M. Kameda, K. Itoh, *J. Org. Chem.* **1999**, *64*. 2178.

[5] a) A. Behr, U. Freudenberg, W. Keim, *J. Mol. Catal.* **1986**, *35*, 9; b) B. Radetich, T. V. RajanBabu, *J. Am. Chem. Soc.* **1998**, *120*, 8007.

[6] a) P. Kisanga, L. A. Goj, R. A. Widenhoefer, *J. Org. Chem.* **2001**, *66*, 635; b) K. L. Bray, I. J. S. Fairlamb, J.-P. Kaiser, G. C. Lloyd-Jones, P. A. Slatford, *Topics in Catalysis* **2002**, *19*, 49; c) K. L. Bray, J. P. H. Charmant, I. J. S. Fairlamb, G. C. Lloyd-Jones, *Chem. Eur. J.* **2001**, *7*, 4205. The use of Pd in ionic liquids has been described, see: d) A. Corma, H. García, A. Leyva, *J. Organomet. Chem.* **2005**, *690*, 3529. The use of Pd in super-critical CO_2 has also been described, see: e) M. Alvaro, D. Das, H. García, A. Leyva, *Tetrahedron* **2004**, *60*, 8131.

[7] a) W. D. Kerber, M. R. Gagné, *Org. Lett.* **2005**, *7*, 3379; b) W. D. Kerber, J. H. Koh, M. R. Gagné, *Org. Lett.* **2004**, *6*, 3013; c) J. H. Koh, M. R. Gagné, *Angew. Chem. Int. Ed.* **2004**, *43*, 3459.

[8] a) A. Heumann, M. Moukhliss, *Synlett* **1998**, 1211; b) A. Heumann, M. Moukhliss, *Synlett* **1999**, 268.

[9] a) C. Böing, G. Franciò, W. Leitner, *Chem. Commun.* **2005**, 1456; b) B. Bogdanović, *Adv. Organomet. Chem.* **1979**, *17*, 104.

[10] a) B. M. Trost, D. L. Van Vranken, C. Bingel, *J. Am. Chem. Soc.* **1992**, *114*, 9327; b) I. J. S. Fairlamb, *Synlett* **2002**, 1176; c) B. M. Trost, L. Li, S. D. Guile, *J. Am. Chem. Soc.* **1992**, *114*, 8745.

[11] a) M. K. Grachev, K. L. Anfilov, A. R. Bekker, E. E. Nifantév, *Zh. Obshch. Khim.* **1995**, *65*, 1946; b) M. K. Grachev, N. O. Soboleva, G. I. Kurochkina, L. K. Vasyanina, V. K. Belśkii, E. E. Nifantév, *Russ. J. Gen. Chem.* **2003**, *73*, 903; c) G. I. Kurochkina, M. K. Grachev, A. A. Sutyagin, E. E. Nifantév, *Russ. J. Gen. Chem.* **2003**, *73*, 1945; d) M. T. Reetz, T. Neugebauer, *Angew. Chem. Int. Ed.* **1999**, *38*, 179; e) M. T. Reetz, G. Mehler, *Angew. Chem. Int. Ed.* **2000**, *39*, 3889.

[12] A. S. C. Chan, W. Hu, C.-C. Pai, C.-P. Lau, *J. Am. Chem. Soc.* **1997**, *119*, 9570.

[13] a) N. Derrien, C. B. Dousson, S. M. Roberts, U. Berens, M. Burk, M. J. Ohff, *Tetrahedron: Asymmetry* **1999**, *10*, 3341; b) B. Adger, U. Berens, M. J. Griffiths, M. J. Kelly, R. McCague, J. A. Miller, C. F. Palmer, S. M. Roberts, R. Selke, U. Vitinus, G. Ward, *Chem. Commun.* **1997**, 1713.

[14] The preliminary cycloisomerisation data for complexes **4a–d**, generated *in situ*, has been reported, see: I. J. S. Fairlamb, S. Grant, A. C. Whitwood, J. Whitthall, A. S. Batsanov, J. C. Collings, *J. Organomet. Chem.* **2005**, *690*, 4462.

[15] K. L. Bray, I. J. S. Fairlamb, G. C. Lloyd-Jones, *Chem. Commun.* **2001**, 187.

[16] Purity was determined to be > 98% as shown by ^{1}H NMR spectroscopy. Contains a trace quantity of dimethylallyl malonate (1.3%; determined by integration of the methyl ester resonances at $\delta=3.71$).

[17] a) A. Fürstner, F. Stelzer, H. Szillat, *J. Am. Chem. Soc.* **2001**, *123*, 11863; b) S. Yamazaki, K. Yamada, K. Yamamoto, *Org. Biomol. Chem.* **2004**, *2*, 257; c) B. B. Snider, D. M. Roush, *J. Org. Chem.* **1979**, *44*, 4229; d) S. Yamazaki, K. Yamada, T. Otsubo, M. Haruna, E. Kutsuwa, H. Tamura, *Chem. Commun.* **2001**, 69; e) S. Yamazaki, S. Inakoa, K. Yamada, *Tetrahedron Lett.* **2003**, *44*, 1429; f) S. Yamazaki, K. Yamada, S. Yamabe, K. Yamamoto, *J. Org. Chem.* **2002**, *67*, 2889.

[18] W. E. Fristad, S. S. Hershberger, *J. Org. Chem.* **1985**, *50*, 1026.
[19] The X-ray data for **12** have been deposited at the Cambridge Crystallographic Database (CCDC 612592). **Crystal data:** *Colourless crystals*, $C_9H_{12}O_4$, M = 184.19, tetragonal (trapezohedral), $a = 6.3896(6)$, $b = 6.3896(6)$, c, 22.023(4) Å, $U = 899.1(2)$ Å^3, $T = 100(2)$ K, $\lambda = 0.71073$ Å, space group $P4_32_12$, $Z = 4$, μ(Mo-K$_a$) = 0.107 mm^{-1}, 5016 reflections measured, 513 unique ($R_{int} = 0.0466$) which were used in all calculations. Final $R1 = 0.041$ and $wR(F^2) = 0.1408$ (all data).
[20] K. M. Kadish, J. E. Anderson, *Pure Appl. Chem.* **1987**, *59*, 703, and references cited therein. Note that this reference provides details of the major impurities found in several chlorinated solvents and methods for their purification.
[21] a) G. Y. Li, *Angew. Chem. Int. Ed.* **2001**, *40*, 1513; b) C. Wolf, R. Lerebours, *J. Org. Chem.* **2003**, *68*, 7077.
[22] I. Pryjomsk, H. Bartosz-Bechowski, Z. Ciunik, A. M. Trzeciak, J. J. Ziółkowski, *Dalton Trans.* **2006**, 213.
[23] a) D. R. Evans, M. Huang, J. C. Fettinger, T. L. Williams, *Inorg. Chem.* **2002**, *41*, 5986; b) T. Ghaffar, A. Kieszkiewicz, S. C. Nyburg, A. W. Parkins, *Acta Crystallogr., Sect. C* **1994**, *50*, 697.
[24] No special precaution was taken to dry the deuterated solvents as we wished to accurately reflect the conditions used in the 1,6-diene cycloisomerisation reaction.
[25] The X-ray data for **30b** have been deposited at the Cambridge Crystallographic Database (CCDC 612591). **Crystal data:** *Clear yellow crystals*, $C_{68}H_{64}Cl_{14}F_6O_{10}P_4Pd_2S_2$, M = 2052.29, triclinic, $a = 11.7768(10)$, $b = 13.1639(11)$, c, 14.1752(12) Å, $U = 2044.2(3)$ Å^3, $T = 115(2)$ K, $\lambda = 0.71073$ Å, space group P-1, $Z = 1$, μ(Mo-K$_a$) = 1.094 mm^{-1}, 19215 reflections measured, 8872 unique ($R_{int} = 0.0460$) which were used in all calculations. Final $R1 = 0.0466$ and $wR(F^2) = 0.1040$ (all data).
[26] Full details of this dimeric Pd(0) structure will be reported in due course: I. J. S. Fairlamb, S. Tommasi, M. Bandini, B. E. Moulton, A. C. Whitwood, unpublished results.
[27] a) Z. Grudzinski, S. M. Roberts, *J. Chem. Soc., Perkin Trans. 1* **1975**, 1767; b) S. M. Ali, N. M. Crossland, T. V. Lee, S. M. Roberts, R. F. Newton, *J. Chem. Soc., Perkin Trans. 1* **1979**, 122; c) E. Marotta, B. Piombi, P. Righi, G. Rosini, *J. Org. Chem.* **1994**, *59*, 7526; d) A. Brown, R. Glen, P. Murray-Rust, J. Murray-Rust, R. F. Newton, *J. Chem. Soc., Chem. Commun.* **1979**, 1178.
[28] a) P. W. N. M. Van Leuween, P. Dierkes, *J. Chem. Soc., Dalton Trans.* **1999**, 1519; b) P. W. N. M. Van Leuween, P. C. J. Kamer, J. N. H. Reek, P. Dierkes, *Chem. Rev.* **2000**, *100*, 2741; c) P. C. J. Kamer, P. W. N. M. van Leuween, J. N. H. Reek, *Acc. Chem. Res.* **2001**, *34*, 895; d) M. Kranenburg, Y. E. M. van der Burgt, P. C. J. Kamer, P. W. N. M. van Leuween, K. Goubitz, J. Fraanje, *Organometallics* **1995**, *14*, 3081; e) P. W. M. N. Van Leuween, P. C. Kamer, J. N. H. Reek, *Pure Appl. Chem.* **1999**, *71*, 1443.
[29] a) J. W. Raebiger, A. Miedaner, A. J. Curtis, A. M. Miller, O. P. Anderson, D. L. Dubois, *J. Am. Chem. Soc.* **2004**, *126*, 5502; b) H. Guan, M. Iimura, M. P. Magee, J. R. Norton, K. E. Janak, *Organometallics* **2003**, *22*, 4084; c) D. E. Berning, B. C. Noll, D. L. DuBois, *J. Am. Chem. Soc.* **1999**, *121*, 11432; d) D. E. Berning, A. Miedaner, C. J. Curtis, B. C. Noll, M. C. Rakowski, D. L. Dubois, *Organometallics* **2001**, *20*, 1832; e) C. J. Curtis, A. Miedaner, W. W. Ellis, D. L. Dubois, *J. Am. Chem. Soc.* **2002**, *124*, 1918.
[30] P. Kisanga, R. A. Widenhoefer, *J. Am. Chem. Soc.* **2000**, *122,* 10017.
[31] The reaction is catalysed slowly by HBF_4 (10 mol%), in the absence of palladium, giving **2c** exclusively (25%).
[32] P. Kisanga, L. A. Goj, R. A. Widenhoefer, *J. Org. Chem.* **2001**, *66*, 635.
[33] a) M. Brookhart, B. Grant, A. F. Volpe, *Organometallics* **1992**, *11*, 3920; b) N. A. Yakelis, R. G. Bergmann, *Organometallics* **2005**, *24*, 3579.
[34] a) H. Günther, *NMR spectroscopy*, 2nd Edition, John Wiley and Sons, Chichester, **1995**, p. 66; b) A. L. Van Geet, *Anal. Chem.* **1968**, *42*, 2227.
[35] a) A. D. Becke, *J. Chem. Phys.* **1993**, *98*, 5648; b) B. Miehlich, A. Savin, H. Stoll, H. Preuss, *Chem. Phys. Lett.* **1989**, *157*, 200; c) C. Lee, W. Yang, G. Parr, G. *Phys. Rev.* **1988**, *B37*, 785.
[36] a) W. R. Wadt, P. J. Hay, *J. Chem. Phys.* **1985**, *82*, 284; b) P. J. Hay, W. R. Wadt, *J. Chem. Phys.* **1985**, *82*, 299.
[37] P. C. Hariharan, J. A. Pople, J. A. *Theor. Chim. Acta* **1973**, *28*, 213.
[38] *Gaussian 03*, revision B05; Gaussian, Inc.: Pittsburgh, PA, **2003**.

